Network structure underlying resolution of conflicting nonverbal and verbal social information

Takamitsu Watanabe[1], Noriaki Yahata[5], Yuki Kawakubo[3], Hideyuki Inoue[2], Yosuke Takano[2], Norichika Iwashiro[2], Tatsunobu Natsubori[2], Hidemasa Takao[4], Hiroki Sasaki[4], Wataru Gonoi[4], Mizuho Murakami[4], Masaki Katsura[4], Akira Kunimatsu[4], Osamu Abe[4,6], Kiyoto Kasai[2], and Hidenori Yamasue[2,7,*]

Departments of [1]Physiology, [2]Neuropsychiatry, [3]Child Neuropsychiatry, and [4]Radiology, Graduate School of Medicine, and [5]Global Center of Excellence (COE) Program "Comprehensive Center of Education and Research for Chemical Biology of the Diseases", The University of Tokyo, 7-3-1 Hongo, Bunkyo-ku, Tokyo 113-8655, Japan
[6]Department of Radiology, Nihon University School of Medicine, 30-1 Oyaguchi kami-cho, Itabashi-ku, Tokyo 173-8610, Japan.
[7]Japan Science and Technology Agency, CREST, 5 Sambancho, Chiyoda-ku, Tokyo, 102-0075, Japan

*Corresponding author: H Yamasue
Department of Neuropsychiatry, Graduate School of Medicine, The University of Tokyo 7-3-1 Hongo, Bunkyo-ku, Tokyo 113-8655, Japan
E-mail: yamasue-tky@umin.ac.jp

Short Title: Neural Network for Social Conflict Resolution
Key Words: Human, Brain, Theory of Mind, Empathy, PPI, Conflict Monitoring

Abstract

Social judgments often require resolution of incongruity in communication contents. Although previous studies revealed that such conflict resolution recruits brain regions including the medial prefrontal cortex (mPFC) and posterior inferior frontal gyrus (pIFG), functional relationships and networks among these regions remain unclear. In this functional magnetic resonance imaging study, we investigated the functional dissociation and networks by measuring human brain activity during resolving incongruity between verbal and nonverbal emotional contents. First, we found that the conflict resolutions biased by the nonverbal contents activated the posterior dorsal mPFC (post-dmPFC), bilateral anterior insula, and right dorsal pIFG, whereas the resolutions biased by the verbal contents activated the bilateral ventral pIFG. In contrast, the anterior dmPFC (ant-dmPFC), bilateral superior temporal sulcus, and fusiform gyrus were commonly involved in both of the resolutions. Second, we found that the post-dmPFC and right ventral pIFG were hub regions in networks underlying the nonverbal- and verbal-content-biased resolutions, respectively. Finally, we revealed that these resolution-type-specific networks were bridged by the ant-dmPFC, which was recruited for the conflict resolutions earlier than the two hub regions. These findings suggest that, in social conflict resolutions, the ant-dmPFC selectively recruits one of the resolution-type-specific networks through its interaction with resolution-type-specific hub regions.

Introduction

Real life is filled with two-sided social information, such as irony and humor, whose nonverbal and verbal contents are in conflict (Pexman 2008), and the incongruity needs to be instantly resolved for adequate social judgments. A series of studies have suggested that this fundamental social ability involves various brain regions such as the medial prefrontal cortex (mPFC), posterior inferior frontal gyrus (pIFG), and superior temporal sulcus (STS) (Amodio and Frith 2006; Zaki and Ochsner 2009): By using social information whose visual and verbal contents are incongruent, prior functional magnetic resonance imaging (fMRI) studies have shown that the mPFC is activated during resolution of the visual-verbal incongruent information (Etkin et al. 2006; Zaki et al. 2010). Other neuroimaging studies have reported increase in the activity of the pIFG and STS as well as the mPFC when subjects are presented with conflicting or ambiguous social stimuli (Decety and Chaminade 2003; Hsu et al. 2005; Mitchell et al. 2006; Wittfoth et al. 2010; Klasen et al. 2011). Other fMRI and electrophysiological studies have demonstrated that the STS is involved in integration of different types of social information (Beauchamp et al. 2004; Ghazanfar et al. 2008).

Although these studies have listed the brain regions related to the social conflict resolution and some of them have reported local interactions among the regions (Etkin et al. 2006; Zaki et al. 2010), detailed functional relationships and network architecture among the brain regions are still elusive. Consequently, it remains unclear either which of the regions mainly controls the social conflict resolutions or which of the connectivity among the regions is selectively recruited in specific conflict resolutions. In this fMRI study, hence, we aimed at clarifying what functional dissociations and network structure among the brain regions are underlying the resolution of social conflict between verbal and nonverbal emotional contents.

For this purpose, we adopted a psychological task that has enabled us to detect brain responses specific to autism spectrum disorders in our recent case-control study

(Watanabe et al. 2012b). This psychological task (Fig. 1A) consists of a series of "friend or foe" judgment tasks, which is considered to recruit brain regions similar to those recruited by social conflict resolutions in real-life situation (Adolphs 2010). The subjects were instructed to make the friend/foe judgments on each person who appeared in each realistic short movie in which different professional actors spoke different emotional words (positive/negative verbal cue) (Bradley and Lang 1999) with different emotional facial expressions and voice prosody (positive/negative nonverbal cue) (Fig. 1B). The movies, therefore, consist of four types of stimuli (Fig. 1B): a positive verbal cue with a positive nonverbal cue (V+NV+), a positive verbal cue with a negative nonverbal cue (V+NV-), a negative verbal cue with a negative nonverbal cue (V-NV-), and a negative verbal cue with a positive nonverbal cue (V-NV+). To reduce the Stroop effect that has been examined in a line of previous studies (Egner and Hirsch 2005; Etkin et al. 2006; Wang et al. 2006; Morishima et al. 2010; Shibata et al. 2010; Ovaysikia et al. 2011), the subjects were allowed to freely make the friend/foe judgments.

To investigate functional dissociations among the relevant brain regions, we classified the subjects' judgments on the incongruent stimuli into verbal- or nonverbal-cue-biased resolutions on the basis of the type of information that mainly affected the friend/foe judgments. For example, a judgment of foe on an actor in a V+NV- movie is regarded as a nonverbal-information-biased resolution (NV resolution), whereas a judgment of friend on an actor in V+NV- movie is considered as a verbal-information-biased resolution (V resolution). In the following analyses, by estimating psychophysiological interactions (PPI) among the relevant brain regions, we depicted detailed network structures among the regions related to social conflict resolutions. Furthermore, by employing a multivariate pattern analysis (MVPA), we investigated which brain regions in the network played a regulatory role in the social conflict resolutions.

Materials and Methods

Subjects

We conducted two fMRI experiments (I and II) by employing two different groups of healthy subjects. The fMRI experiment I employed 27 subjects (11 female, mean age = 27.3, range: 21–36). The fMRI experiment II recruited 7 subjects (three female, mean age = 26.4, range: 24–29). All the subjects were Japanese and right-handed. The handedness indices of all the subjects were over 80 in the Edinburgh handedness inventory (Oldfield 1971). None of the subjects had a history of neuropsychiatric disorder. The ethics committee of The University of Tokyo Hospital approved this study (#1350). Written informed consents were obtained from all the subjects.

Task and MRI scanning

The task and stimuli were exactly the same as those used in our recent case-control study (Watanabe et al. 2012b) (Fig. 1A, Fig. 1B, Supplementary Movies S1–4, Supplementary Methods). We used a 3T MRI scanner (General Electric, CT, USA) with a magnet-compatible headphone system (Hitachi, Corp. Tokyo, Japan). fMRI images were obtained by gradient-echo echo-planar sequences (TR = 3 s, TE = 35 ms, flip angle = 80 degrees, 4×4×4 mm, 22 slices, interleaved acquisition), whose first five images in each run were excluded from the analysis to account for the equilibrium of longitudinal magnetization.

Behavioral analyses for the fMRI experiment I

In the behavioral analyses for the fMRI experiment I, we first conducted a paired t-test to compare the response time between the congruent and incongruent stimuli trials. We then examined the differences in response time between the V and NV resolution trials. The

possible effects of conflict adaptation were also tested (Logan and Zbrodoff 1979; Gratton et al. 1992; Egner and Hirsch 2005). We then evaluated effects of first impressions on the following judgments (Schiller et al. 2009). For example, if a subject had a positive first impression of an actor, the subject might tend to judge the following movies of the same actor in a positive way. To estimate the effect, we compared the proportions of positive (friend) and negative (foe) judgments of the incongruent movie that followed the first congruent movie. Finally, the number of the NV resolution trials was compared with that of the V resolution trials using a paired t-test.

Neuroimaging analysis of the fMRI experiment I

The data were analyzed using SPM8 (http://www.fil.ion.ucl.ac.uk/spm/). Functional images were realigned, slice timing corrected, normalized to the default template with interpolation to a 2×2×2 mm space, and smoothed (FWHM = 8 mm, Gaussian filter). High-pass temporal filtering with a cut-off of 128 s was applied. In single-level analyses, we used a general linear model with the following regressors: two regressors for the congruent trials (Friend to V+NV+ and Foe to V-NV-), and four regressors for two types of the incongruent stimuli (V+NV- and V-NV+) × two types of the judgment (Friend and Foe). In the regressors, each of the trials were coded at each stimulus onset with duration time equal to each of the response time. To use the brain activity during direct response to the congruent stimuli as a baseline of the activity, we excluded a small number of non-straight responses to the congruent stimuli (i.e. Friend to V-NV- and Foe to V+NV+). After the single level analyses, based on a random-effects model, we conducted group analyses across subjects with a threshold of $P < 0.05$ (FDR-corrected, revised version in the latest SPM8) (Chumbley and Friston 2009).

To identify brain regions that were specifically activated during V resolution or NV resolution, we conducted the whole-brain repeated-measure two-way analysis of variance (ANOVA) of the fMRI signals (type of resolutions: V resolution/NV resolution × type of judgments: Friend/Foe), and estimated the main effect of the type of resolutions. We denoted these brain regions specific to V or NV resolution as V Region or NV Regions, respectively (Fig. 2A and 2B).

To investigate brain regions that were commonly activated in both types of conflict resolutions, we employed a conjunction analysis of V resolution trials and NV resolution trials (Nichols et al. 2005; Chadick and Gazzaley 2011; Daw et al. 2011; Kahnt et al. 2011; Klasen et al. 2011; Xue et al. 2011). Based on the standard procedure of the conjunction analysis with conservative null hypothesis (Nichols et al. 2005), we first estimated a whole brain map for V resolution trails ("Friend to V+NV- > Friend to V+NV+" and "Foe to V-NV+ > Foe to V-NV-"), and a whole brain map for NV resolution trials ("Foe to V+NV- > Foe to V-NV-" and "Friend to V-NV+ > Friend to V+NV+"). Note that brain regions in these two brain maps were different from V Region and NV Region. We then converted the two brain maps to two binary maps by using $P < 0.001$ uncorrected as a threshold (Klasen et al. 2011). By multiplying the two binary maps, we obtained a whole brain map indicating a conjunction of the two conditions ($P < 10^{-6}$, uncorrected). We denoted these regions commonly involved in both types of resolutions as V&NV Regions (Fig. 2C).

To estimate the influence of unbalance between the number of V and NV trials on these activation results, we conducted the two different analyses. (1) In the group-level analysis, we newly adopted the number of V and NV trials for each of the subjects as covariates. The other parts of the analyses were the same as the original manner. (2) In the single-subject-level analysis, we made the number of NV trials same as that of V trials by the random sampling as follows: For subjects whose number of NV trials was larger than that of

V trials, we randomly selected the same number of the NV trials as that of the V trials. For subjects whose number of V trials was larger than that of NV trials, we randomly selected the same number of the V trials as that of the NV trials. The other parts of the analyses were the same as the original manner.

PPI analysis and comparison with behavioral patterns

We then estimated the PPIs (Büchel and Friston 1997; Etkin et al. 2006; Watanabe et al. 2012a) among two sets of the brain regions based on implementation in SPM8 (Friston et al. 1997): the first set consisted of V Regions and V&NV Regions, and the other set consisted of NV Regions and V&NV Regions. In a single subject level estimation, each fMRI signal was defined as an averaged value in a 4-mm-radius sphere in each region (Morishima et al. 2010). Each psychological factor was defined as a regressor contrasting V resolution trials and NV resolution trials. For example, PPIs among V Regions and V&NV Regions were calculated as enhanced functional interaction during V resolution trials than NV resolution trials. The individual results were submitted to a random-effects group analysis using one-sample t-tests. We evaluated PPIs for all the possible connections among each set of regions, and estimated their statistical power using a rough-FDR correction for multiple comparisons.

Based on the network topology based on the PPI analysis, we calculated degree centrality (i.e., the number of significantly enhanced PPIs) for all the related regions (Sporns et al. 2007; Bullmore and Sporns 2009; Zuo et al. 2011), and identified resolution-type-specific hub regions and the resolution-type-general central region. For functional characterization, we then estimated Pearson's correlation coefficients across subjects between the brain activity of the brain regions and two behavior scores: the number of trials for the corresponding types of resolutions, and the response time for the resolutions.

Neuroimaging analysis of the fMRI experiment II

To avoid a circular analysis and maintain the independence of this analysis from the aforementioned analysis, we employed independent seven subjects who did not undergo the fMRI experiment I. The new seven subjects underwent the same psychological task as in the fMRI experiment I with the same fMRI scanning setting. We applied the same preprocessing to the obtained fMRI images as in the analysis for the fMRI experiment I, except smoothing, which is not suitable for the following MVPA (Watanabe et al. 2011).

MVPA-based characterization of resolution-type-specific hub regions

We first examined whether the brain activity in the resolution-type-specific hub regions had enough information to accurately classify responses to the incongruent stimuli to V resolutions or NV resolutions. In a single subject level, to evaluate the fMRI signal in each trial independently of behavior, we set a different regressor for each trial in a GLM (i.e., 80 regressors were built into the GLM for 80 trials) (Polyn et al. 2005; Johnson et al. 2009; Schurger et al. 2010; Watanabe et al. 2011). To minimize the temporal interaction among adjacent trials, the resulting GLM was corrected for temporal autocorrelations using a first-order autoregressive model. For each trial involving the incongruent stimuli, we extracted averaged signals in the resolution-type-specific hub regions, whose coordinates were based on the fMRI experiment I. Consequently, 40 sets of the fMRI signals in the 40 incongruent trials were obtained and were submitted into MVPA. In the MVPA, using a linear support vector machine (SVM) (Haynes and Rees 2005; Kamitani and Tong 2005; Watanabe et al. 2011), we used the sets of fMRI signals as features and the corresponding labels (V resolutions or NV resolutions) as classes. We first used 39 of the 40 sets of the fMRI signals to train the linear SVM, and then tested the trained SVM using the rest of the 40 sets of the fMRI signals. We repeated this training and test procedure 40 times, and estimated how many

of the responses were accurately predicted (leave-one-out cross-validation test, LOOCV test) (Kamitani and Tong 2005; 2006; Pereira et al. 2009). The statistical significance for accuracy was evaluated in a permutation test (Pereira et al. 2009; Schurger et al. 2010; Watanabe et al. 2011).

MVPA-based time course analysis of the three central regions

We next investigated the temporal relationship between the resolution-type-general central region and resolution-type-specific hub regions by estimating the time course of the classification accuracy in MVPA (Polyn et al. 2005; Johnson et al. 2009; Watanabe et al. 2011). By building independent regressors, we divided time of 6 s from the stimulus onset into six time periods, and extracted fMRI signals during each of the time periods around the coordinates of these central regions, which were determined in the fMRI experiment I. By using another MVPA employing a linear SVM, we estimated how accurately the fMRI signals in each of the six time periods classified the fMRI signals into the congruent and incongruent trials as follows.

As in previous studies (Polyn et al. 2005; Johnson et al. 2009; Schurger et al. 2010; Watanabe et al. 2011), we first built six box-car-type sequential regressors with length of 1.0 s for each of the stimuli (i.e., overall, 6 × 80 regressors of interest). Using these regressors, we conducted a general linear model (GLM) in a single subject level. To minimize the temporal interaction among adjacent trials, the resulting GLM was corrected for temporal autocorrelations using a first-order autoregressive model. Through these processes, we obtained fMRI signals representing the corresponding time period of 1.0 s (i.e., from the onset of the stimuli to 6 s after the stimulus onset). By using MVPA, we next searched for which of the fMRI signals in the six time periods had the largest information to classify the congruent and incongruent trials. As an example, we will explain the procedure for the case

of the fMRI data during the first time period (i.e., 0–1.0 s from the stimulus onset) in the resolution-type-general central region (i.e., the ant dmPFC). (i) We collected the fMRI data for the first time period for all the 80 trials. (ii) For each of the data, we extracted sets of fMRI signals in the 33 voxels around the coordinates of the ant dmPFC, which was independently determined in the fMRI experiment I (33 voxels are equivalent to voxels in the sphere with radius of 5 mm) (Watanabe et al. 2011). Consequently, we obtained 40 sets of 33 voxels of fMRI signals during the congruent trials and 40 sets during the incongruent trials. (iii) Using 79 sets of the data, we trained a linear SVM, and tested the trained linear SVM by using the rest of the data set. We repeated this training and test procedure 80 times (LOOCV). (iv) We estimated how many trials the linear SVM accurately classified into the congruent or incongruent trials, and obtained classification accuracy. The significance for the accuracy was evaluated in a permutation test.

We applied these steps to all the six time periods in all the three central regions, and obtained the time course of classification accuracy for all the regions in one subject. We then repeated this procedure in all the seven subjects in experiment II, and conducted across-subject paired t-tests of the accuracy in each time period between the resolution-type-general central region and resolution-type-specific hub regions.

Results

Behavioral results

The subjects responded in a straightforward manner to almost all the congruent stimuli. Almost all of the V-NV-stimuli were judged as foe (94.0 ± 6.0 %, mean ± s.d.), while almost all the V+NV+ stimuli as friend (90.0 ± 11.0 %). In the incongruent stimuli trials, the response time was significantly longer than that in the congruent stimuli trials ($t(26) = 6.50$, $P < 0.01$, paired t-test; Fig. 1C), validating that the subjects were conducting conflict resolution

in the incongruent stimuli trials. The subjects showed significantly more NV resolutions than V resolutions ($t(26) = 6.97$, $P < 0.001$, paired t-test; Fig. 1D). However, the response time did not show a significant difference between the two types of the conflict resolutions ($P > 0.5$, paired t-test; Fig. 1E).

The effect of the first impression (Schiller et al. 2009) could be excluded because there was no significant difference in tendency of the friend/foe judgments on the later movies between different initial movies ($P > 0.5$, paired t-test). Moreover, the effect of conflict adaptation (Logan and Zbrodoff 1979; Gratton et al. 1992; Egner and Hirsch 2005) was evaluated through comparison of response time for the incongruent stimuli following the congruent stimuli with that for the incongruent stimuli following other incongruent stimuli. We did not find a significant difference in the paired t-test across subjects ($P > 0.21$), allowing us to exclude a possible effect of conflict-adaptation in the following analyses.

Brain regions specific to V or NV resolutions

To identify brain regions specific to V or NV resolutions, we conducted the whole-brain repeated-measure two-way ANOVA of the fMRI signals during the incongruent stimuli trials (type of judgments: Friend/Foe × type of resolutions: V/NV resolution), and estimated the main effect of the type of resolutions. We found that the posterior dorsal mPFC (post-dmPFC), bilateral anterior insula (AI), and right dorsal pIFG showed significantly larger activity during NV resolutions than during V resolutions, whereas the bilateral ventral pIFG showed significantly larger activity during V resolutions than during NV resolutions ($P < 0.05$, FDR-corrected; Fig. 2A and 2B; Table 1). In contrast, we found neither a significant main effect of type of judgments nor a significant interaction in any brain region. In the following sections, the regions specific to V resolution are denoted by V Regions, and those specific to NV resolution are denoted by NV Regions.

To examine effects of the unbalanced number between V and NV trials on these results, we conducted two different analyses (*see* Methods). One of the analyses used the number of V and NV trials as covariates in the group-level analysis, and the other was based on random sampling similar to Monte-Carlo method. Although the coordinates of the brain regions were slightly fluctuated, both of the analyses essentially replicated the original results (Supplementary Table S1 and S2).

Brian regions common to V and NV resolutions

We then aimed at identifying brain regions commonly involved in V and NV resolutions through a conjunction analysis of V-resolution-related regions ($P < 0.001$, uncorrected) and NV-resolution-related regions ($P < 0.001$, uncorrected) with a conservative null hypothesis (Nichols et al. 2005). The statistical threshold in this conjunction analysis is $P < 10^{-6}$, which is strict enough in the whole brain analysis (Chadick and Gazzaley 2011). Note that the V or NV-resolution-related regions are not the same as V or NV Regions. The V or NV-resolution-related regions were considered to consist of not only resolution-type-specific regions, but also resolution-type-common regions. Consequently, we found the anterior dmPFC (ant-dmPFC), bilateral fusiform gyrus, and bilateral STS (Fig. 2C). Their coordinates in Table 1 represent the approximate center coordinates. Hereafter, these regions are denoted by V&NV Regions.

Network architecture underlying conflict resolutions

To reveal the network architectures underlying the social conflict resolutions, we then conducted PPI analyses among the found brain regions. For the V-resolution-specific network consisting of V Regions and V&NV Regions, six PPIs were significantly enhanced during V resolution trials compared with NV resolution trials ($P < 0.05$, FDR-corrected

among 42 potential PPIs; Fig. 3A, Table 2). For the NV-resolution-specific network consisting of NV Regions and V&NV Regions, other six PPIs were enhanced during NV resolution trials compared with V resolution trials ($P < 0.05$, FDR-corrected among 72 potential PPIs; Fig. 3A, Table 2). Based on these PPI analyses, we compared degree centrality of each region (i.e., the number of significant PPIs connecting to the region). Consequently, the right ventral pIFG had the largest degree centrality among V Regions, the post-dmPFC had among NV Regions, and the ant-dmPFC had among V&NV Regions (Fig. 3B). Moreover, these three high-degree regions had direct connections with each other (Fig. 3A).

These results suggest that the right ventral pIFG is a hub region in the V-resolution-specific neural network, whereas the post-dmPFC is a hub region in the NV-resolution-specific neural network. Moreover, these results also allow us to hypothesize that the ant-dmPFC plays a regulatory role by bridging the two resolution-type-specific hub regions.

Comparison with behavioral patterns

We examined the hypothesized central roles of the right ventral pIFG, post-dmPFC, and ant-dmPFC by comparing the brain activity with corresponding behavioral patterns. First, a significantly positive correlation was found between the fMRI signal in the right ventral pIFG and the number of V resolution ($P < 0.05$, Bonferroni-corrected among V Regions; left panel in Fig. 3C). Another significant positive correlation was also found between the fMRI signal in the post-dmPFC and the number of NV resolution ($P < 0.05$, Bonferroni-corrected among NV Regions; right panel in Fig. 3C). We did not find any significant correlation in the other V, NV, V&NV Regions. These results suggest that, compared with the other brain regions,

the activity of the hub regions have more influence on the social conflict resolutions, which is consistent with the network structure presented in the above analysis.

Moreover, we found significantly positive correlations with the response time spent for friend/foe judgments only in the ant-dmPFC in both types of resolutions ($P < 0.05$, Bonferroni-corrected among V&NV Regions; Fig. 3D). This result suggests that the ant-dmPFC is involved in the general process of the social conflict resolutions, which is consistent with the network topology revealed in the above PPI analysis.

MVPA-based characterization of the resolution-type-specific hub regions

To confirm that the activity in the resolution-type-specific hub regions is strongly associated with the type of resolution, we conducted a MVPA using a different set of the subjects (fMRI experiment II), and tested whether the brain activity in the resolution-type-specific hub regions accurately predicts resolution type for each of the incongruent stimuli in a trial-by-trial manner. Consequently, we could predict types of resolutions in a single trial level in all the seven new subjects with significantly high accuracy ($P < 0.05$, a permutation test; a representative result shown in Fig. 4A; results of all the seven subjects shown in Fig. 4B). We could not predict with significantly high accuracy by using the other possible combinations of brain activity in the V Regions and NV Regions ($P > 0.4$). These results validate that the post-dmPFC and right ventral pIFG play central roles in each resolution-type-specific neural network.

MVPA-based time-course analysis

These results of the PPI analyses and comparison with behavioral patterns imply a certain special role of the ant-dmPFC among V&NV Regions. To further investigate the role, by using another MVPA, we compared the time course of classification accuracy of the ant-

dmPFC with those of the resolution-type-specific hub regions (i.e., the right ventral pIFG and post-dmPFC) (Polyn et al. 2005; Johnson et al. 2009; Watanabe et al. 2011). Consequently, as shown in Fig. 4C, the brain activity in the ant-dmPFC had the largest information to classify the congruent and incongruent stimuli trials at 2 s after the stimulus onset ($P < 0.0001$ in a permutation test). In contrast, the brain activity in the resolution-type-specific hub regions had the largest information at 4 s after the onset ($P < 0.0001$ in a permutation test). The classification accuracy based on the ant-dmPFC was significantly higher at 2 s after the onset than those based on the right ventral pIFG/post-dmPFC ($t(6) > 12.4$, $P < 0.05$, Bonferroni-corrected, paired t-tests). The accuracy at 4 s after the onset showed the opposite pattern ($t(6) > 11.9$, $P < 0.05$, Bonferroni-corrected, paired t-tests). These results suggest that the ant-dmPFC responds to incongruent stimuli earlier than the resolution-type-specific hub regions, and imply that the ant-dmPFC regulates which of the resolution-type-specific neural networks is recruited through the interactions with the hub regions.

Discussion

The current study demonstrated the structure of the neural network underlying the resolution of verbal/nonverbal incongruent social information by employing correlational analyses with behavior, PPI analysis, and MVPAs. The network structure contains two resolution-type-specific sub-networks: The sub-network for the V resolutions involves the right ventral pIFG as a hub region, whereas the sub-network for the NV resolutions involves the post-dmPFC as a hub. The two sub-networks are bridged by the resolution-type-general ant-dmPFC, which interacts with both of the resolution-type-specific hub regions. In addition, the MVPA-based time course analysis implies that the ant-dmPFC regulates the resolution-type-specific hub regions.

In the present study, we built up the resolution-type-specific networks from the

brain regions whose activity was significantly increased during the conflict resolutions. Therefore, there is a reasonable possibility that, even if their activity was not large enough, other brain regions are linked with the networks. Indeed, in whole-brain-level analyses of resolution-type-specific PPIs, we found several brain regions whose PPIs with the corresponding resolution-type-specific hub region were significantly enhanced (Supplementary Fig. S1 and Table S3): First, commonly in the V-resolution-specific and NV-resolution-specific networks, we observed significant enhancement in functional connectivity from the corresponding hub region to the left inferior parietal regions. This result is consistent with a series of previous studies showing that the inferior parietal area is recruited in decision making (Daw et al. 2006; Seo et al. 2009; Vickery and Jiang 2009). Moreover, especially in the V-resolution-specific network, the functional connectivity from the hub region to the left triangular IFG also exhibited significant increase. Based on findings reported in a line of previous studies (Foundas et al. 1996; Badre et al. 2005; Saur et al. 2008), the functional connectivity with the triangular IFG was recruited specifically in the V resolution because the brain region is thought to be deeply related to language-based cognitive process. These results of the whole-brain PPI analyses indicate the necessity of future studies on how the present resolution-type-specific networks are interacting with other brain regions.

By using realistic movie stimuli with professional actors, the present study experimentally captured the neural substrate similar to that believed to underlie social judgments in real life. Most previous studies presented subjects with written sentences rather than vocal information of them, or with nonverbal information in the form of static pictures, cartoons, silent movies, or computer graphics (Eviatar and Just 2006; Wang et al. 2006; Iidaka et al. 2010; Wittfoth et al. 2010; Zaki et al. 2010; Klasen et al. 2011). The current study employed short movies in which trained professional actors displayed emotional facial

expressions while speaking a single negative or positive word with expressive emotional prosody. These realistic video stimuli were chosen to minimize the differences between the psychological task and real-life social situations. This allowed us to experimentally examine the neural basis of incongruity resolution that is close to automatic resolution of incongruent social information in real-life environments.

However, it is also the case that the present psychological task cannot exclude several confounding factors by itself because the friend/foe judgments can be influenced by individual preference and developmental history of each of the subjects. For example, the judgments would be affected by in-group/out-group relationship and trustworthiness of the persons in the stimuli. In addition, according to previous studies (Winston et al. 2002; de Quervain et al. 2004; King-Casas et al. 2005; Hein et al. 2010), these factors are known to influence the brain activity of the regions observed in the present study. Therefore, although all the subjects in our present study and all the actors in the movie stimuli belong to the same race and nationality and seemed to be in the similar social class, further studies using different psychological tasks are necessary to examine whether or not the present neural networks are specific to the verbal-nonverbal social conflict resolution.

The present results indicate the functional dissociation between the anterior and posterior dmPFC during resolution of conflicting social information. Previous studies have demonstrated that the brain area around the ant-dmPFC found in the present study engages in conflict processing and decisions in uncertain situations (Ridderinkhof et al. 2004), as well as in the monitoring of conflicting actions (Amodio and Frith 2006) and conflicting social information (Zaki et al. 2010; Klasen et al. 2011). The brain area around the post-dmPFC has also been shown to be involved in resolution of conflicting social information (Zaki et al. 2010) or audio-visual incongruent information (Klasen et al. 2011). In the present study, both of the regions played regulatory roles, but the post-dmPFC had a resolution-type-specific

function, whereas the ant-dmPFC had a resolution-type-general function. This functional dissociation inside the dmPFC expands the previous findings on the role of the dmPFC during social conflict resolutions.

Our study also revealed extensive interactions between the post-dmPFC and other social cognitive regions during judgments for others' intention. The post-dmPFC has been suggested to have abundant functional and anatomical connections with extensive brain regions including social cognitive networks (Northoff et al. 2006; Heuvel et al. 2008). Previous graph theoretical examinations (Sporns et al. 2007; Hagmann et al. 2008) have suggested that efficient processing in the neural network is promoted in structures interlinked by hub regions such as the medial prefrontal regions. A previous fMRI study on social conflict resolution also indicated that the post-dmPFC interacts with other dmPFC regions (Zaki et al. 2010). The current findings lend further support to the notion that the post-dmPFC plays an essential role as a hub in the social cognitive network.

The present study expands previous knowledge on the differential roles of the vmPFC and dmPFC in processing social information. We found that the vmPFC was strongly activated during the processing of congruent stimuli, whereas the dmPFC was activated during the processing of incongruent stimuli. Previous studies have suggested that the vmPFC engages in self-referential mentalizing (Rilling et al. 2002; 2004; Jenkins and Ranganath 2010; Krienen et al. 2010; Tamir and Mitchell 2010), while the dmPFC is associated with non-self-referential mentalizing and deeper objective reasoning (Mitchell et al. 2006; Coricelli and Nagel 2009; Shamay-Tsoory et al. 2009). Other studies indicate that, compared with the dmPFC, the vmPFC tends to be activated during reward-based decision making (Bush et al. 2002; Williams et al. 2004; Rushworth et al. 2005). Taken together with these previous findings, the present results suggest that the dmPFC plays a role in processing uncertain and complex social information, whereas the vmPFC is involved in processing

familiar and well-known social stimuli that enable subjects to predict reward more easily than unpredictable and complex stimuli.

The current results also suggest different roles of the right dorsal and ventral pIFG in the resolution of incongruent information: the dorsal pIFG appears to be involved in nonverbal-information-biased resolutions, while the ventral pIFG appears to be involved in verbal-information-biased resolutions. These results thus extend the previous understanding of the functional difference between these regions. In language processing, the dorsal pIFG is thought to be involved in phonological and articulatory processing (Morimoto et al. 2008), while the ventral pIFG is involved in semantic processing (Thiebaut de Schotten et al. 2005; Saur et al. 2008; Hagoort and Levelt 2009; Jimura et al. 2009). In the processing of social information, the dorsal pIFG is thought to perform 'mirror' processing, whereas the ventral pIFG is activated only during imitation, and not during observation (Molnar-Szakacs et al. 2005; Iacoboni 2009; Singer and Lamm 2009). Taken together with this previous evidence, the current results suggest that the right dorsal pIFG is mainly involved in the processing of nonverbal interpersonal information through mirroring others' behavior and emotion, whereas the right ventral pIFG is mainly engaged in processing verbal interpersonal information without mirroring others' behavior.

The present results further suggest functional laterality of the pIFG in social incongruity resolution. Previous studies have suggested non-left dominancy in imitative behavior (Aziz-Zadeh et al. 2006) and a significant role of the right pIFG in social behavior (Carr et al. 2003; Yamasue et al. 2008; Yamasaki et al. 2010). The present results indicate that nonverbal-cue-biased resolution for social judgment involves the right pIFG rather than the left pIFG, in accordance with the previous literature.

Overall, the present study depicted the detailed network structure during resolutions of verbal/nonverbal incongruent social information. In the neural network, the

combination of correlational analyses with behavior, PPI analysis, and MVPAs suggest that the resolution-type-general ant-dmPFC controls the two resolution-type-specific hub regions (i.e., the post-dmPFC and right ventral pIFG), and the hub regions might control their corresponding resolution-type-specific neural networks. As suggested in neural networks related to resolution of non-social conflicting information (Botvinick et al. 2001), this network architecture is thought to realize efficient social judgments in the presence of a large amount of conflicting nonverbal and verbal information. We believe that these novel findings will contribute to the understanding of the neural mechanisms underlying social cognition in real life situations.

Acknowledgements.

We thank Dr. Y. Morishima for helpful comments on the manuscript. Part of this study was the result of a project titled the "Development of biomarker candidates for social behavior" carried out under the Strategic Research Program for Brain Sciences by the MEXT, and was also supported by Comprehensive Research on Disability Health and Welfare (to H.Y.), KAKENHI (22689034 to H.Y.), the Global Center of Excellence (COE) Program "Comprehensive Center of Education and Research for Chemical Biology of the Diseases" (N.Y.), and a grant from the Japan Society for the Promotion of Science Research Foundation for Young Scientists to T.W. (222882).

References

Adolphs R. 2010. Conceptual challenges and directions for social neuroscience. Neuron. 65:752–767.

Amodio DM, Frith CD. 2006. Meeting of minds: the medial frontal cortex and social cognition. Nat Rev Neurosci. 7:268–277.

Aziz-Zadeh L, Wilson SM, Rizzolatti G, Iacoboni M. 2006. Congruent embodied representations for visually presented actions and linguistic phrases describing actions. Curr Biol. 16:1818–1823.

Badre D, Poldrack RA, Paré-Blagoev EJ, Insler RZ, Wagner AD. 2005. Dissociable controlled retrieval and generalized selection mechanisms in ventrolateral prefrontal cortex. Neuron. 47:907–918.

Beauchamp MS, Lee KE, Argall BD, Martin A. 2004. Integration of auditory and visual information about objects in superior temporal sulcus. Neuron. 41:809–823.

Botvinick MM, Braver T, Barch D, Carter C, Cohen JD. 2001. Conflict monitoring and cognitive control. Psychol Rev. 108:624–652.

Bullmore E, Sporns O. 2009. Complex brain networks: graph theoretical analysis of structural and functional systems. Nat Rev Neurosci. 10:186–198.

Büchel C, Friston KJ. 1997. Modulation of connectivity in visual pathways by attention: cortical interactions evaluated with structural equation modelling and fMRI. Cereb Cortex. 7:768–778.

Bush G, Vogt BA, Holmes J, Dale AM, Greve D, Jenike MA, Rosen BR. 2002. Dorsal anterior cingulate cortex: a role in reward-based decision making. Proc Natl Acad Sci USA. 99:523–528.

Carr L, Iacoboni M, Dubeau M-C, Mazziotta JC, Lenzi GL. 2003. Neural mechanisms of empathy in humans: a relay from neural systems for imitation to limbic areas. Proc Natl Acad Sci USA. 100:5497–5502.

Chadick JZ, Gazzaley A. 2011. Differential coupling of visual cortex with default or frontal-parietal network based on goals. Nat Neurosci. 14:830–832.

Chumbley JR, Friston KJ. 2009. False discovery rate revisited: FDR and topological inference using Gaussian random fields. NeuroImage. 44:62–70.

Coricelli G, Nagel R. 2009. Neural correlates of depth of strategic reasoning in medial prefrontal cortex. Proc Natl Acad Sci USA. 106:9163–9168.

Daw ND, O'Doherty JP, Dayan P, Seymour B, Dolan RJ. 2006. Cortical substrates for exploratory decisions in humans. Nature. 441:876–879.

Daw ND, Gershman SJ, Seymour B, Dayan P, Dolan RJ. 2011. Model-based influences on humans' choices and striatal prediction errors. Neuron. 69:1204–1215.

Decety J, Chaminade T. 2003. Neural correlates of feeling sympathy. Neuropsychologia. 41:127–138.

de Quervain DJ-F, Fischbacher U, Treyer V, Schellhammer M, Schnyder U, Buck A, Fehr E. 2004. The neural basis of altruistic punishment. Science. 305:1254–1258.

Egner T, Hirsch J. 2005. Cognitive control mechanisms resolve conflict through cortical amplification of task-relevant information. Nat Neurosci. 8:1784–1790.

Etkin A, Egner T, Peraza D, Kandel E, Hirsch J. 2006. Resolving Emotional Conflict: A Role for the Rostral Anterior Cingulate Cortex in Modulating Activity in the Amygdala. Neuron. 51:871–882.

Eviatar Z, Just MA. 2006. Brain correlates of discourse processing: an fMRI investigation of irony and conventional metaphor comprehension. Neuropsychologia. 44:2348–2359.

Friston KJ, Buechel C, Fink GR, Morris J, Rolls ET, Dolan RJ. 1997. Psychophysiological and modulatory interactions in neuroimaging. NeuroImage. 6:218–229.

Foundas AL, Leonard CM, Gilmore RL, Fennell EB, Heilman KM. 1996. Pars triangularis asymmetry and language dominance. Proc Natl Acad Sci USA. 93:719–722.

Ghazanfar AA, Chandrasekaran C, Logothetis NK. 2008. Interactions between the superior temporal sulcus and auditory cortex mediate dynamic face/voice integration in rhesus monkeys. Journal of Neuroscience. 28:4457–4469.

Gratton G, Coles MG, Donchin E. 1992. Optimizing the use of information: strategic control of activation of responses. J Exp Psychol Gen. 121:480–506.

Hagmann P, Cammoun L, Gigandet X, Meuli R, Honey CJ, Wedeen VJ, Sporns O. 2008. Mapping the structural core of human cerebral cortex. PLoS Biol. 6:e159.

Hagoort P, Levelt WJM. 2009. Neuroscience. The speaking brain. Science. 326:372–373.

Haynes J-D, Rees G. 2005. Predicting the orientation of invisible stimuli from activity in human primary visual cortex. Nat Neurosci. 8:686–691.

Hein G, Silani G, Preuschoff K, Batson CD, Singer T. 2010. Neural responses to ingroup and outgroup members' suffering predict individual differences in costly helping. Neuron. 68:149–160.

Heuvel MPVD, Stam CJ, Boersma M, Pol HEH. 2008. Small-world and scale-free organization of voxel-based resting-state functional connectivity in the human brain. NeuroImage. 43:528–539.

Hsu M, Bhatt M, Adolphs R, Tranel D, Camerer CF. 2005. Neural systems responding to degrees of uncertainty in human decision-making. Science. 310:1680–1683.

Iacoboni M. 2009. Imitation, empathy, and mirror neurons. Annu Rev Psychol. 60:653–670.

Iidaka T, Saito DN, Komeda H, Mano Y, Kanayama N, Osumi T, Ozaki N, Sadato N. 2010. Transient neural activation in human amygdala involved in aversive conditioning of face and voice. J Cogn Neurosci. 22:2074–2085.

Jenkins LJ, Ranganath C. 2010. Prefrontal and medial temporal lobe activity at encoding predicts temporal context memory. Journal of Neuroscience. 30:15558–15565.

Jimura K, Yamashita K-I, Chikazoe J, Hirose S, Miyashita Y, Konishi S. 2009. A critical component that activates the left inferior prefrontal cortex during interference resolution. Eur J Neurosci. 29:1915–1920.

Johnson JD, McDuff SGR, Rugg MD, Norman KA. 2009. Recollection, familiarity, and cortical reinstatement: a multivoxel pattern analysis. Neuron. 63:697–708.

Kahnt T, Grueschow M, Speck O, Haynes J-D. 2011. Perceptual learning and decision-making in human medial frontal cortex. Neuron. 70:549–559.

Kamitani Y, Tong F. 2005. Decoding the visual and subjective contents of the human brain. Nat Neurosci. 8:679–685.

Kamitani Y, Tong F. 2006. Decoding seen and attended motion directions from activity in the human visual cortex. Curr Biol. 16:1096–1102.

King-Casas B, Tomlin D, Anen C, Camerer CF, Quartz SR, Montague PR. 2005. Getting to know you: reputation and trust in a two-person economic exchange. Science. 308:78–83.

Klasen M, Kenworthy CA, Mathiak KA, Kircher TTJ, Mathiak K. 2011. Supramodal Representation of Emotions. Journal of Neuroscience. 31:13635–13643.

Krienen FM, Tu P-C, Buckner RL. 2010. Clan mentality: evidence that the medial prefrontal cortex responds to close others. J Neurosci. 30:13906–13915.

Logan GD, Zbrodoff NJ. 1979. When it helps to be misled: Facilitative effects of increasing the frequency of conflicting stimuli in a Stroop-like task. Mem Cognit. 7:166–174.

Mitchell JP, Macrae CN, Banaji MR. 2006. Dissociable medial prefrontal contributions to judgments of similar and dissimilar others. Neuron. 50:655–663.

Molnar-Szakacs I, Iacoboni M, Koski L, Mazziotta JC. 2005. Functional segregation within pars opercularis of the inferior frontal gyrus: evidence from fMRI studies of imitation and action observation. Cereb Cortex. 15:986–994.

Morimoto HM, Hirose S, Chikazoe J, Jimura K, Asari T, Yamashita K-I, Miyashita Y, Konishi S. 2008. On verbal/nonverbal modality dependence of left and right inferior prefrontal activation during performance of flanker interference task. J Cogn Neurosci. 20:2006–2014.

Morishima Y, Okuda J, Sakai K. 2010. Reactive mechanism of cognitive control system. Cerebral Cortex. 20:2675–2683.

Nichols T, Brett M, Andersson J, Wager T, Poline J-B. 2005. Valid conjunction inference with the minimum statistic. NeuroImage. 25:653–660.

Northoff G, Heinzel A, de Greck M, Bermpohl F, Dobrowolny H, Panksepp J. 2006. Self-referential processing in our brain--a meta-analysis of imaging studies on the self. NeuroImage. 31:440–457.

Oldfield RC. 1971. The assessment and analysis of handedness: the Edinburgh inventory. Neuropsychologia. 9:97–113.

Ovaysikia S, Tahir KA, Chan JL, Desouza JFX. 2011. Word wins over face: emotional Stroop effect activates the frontal cortical network. Front Hum Neurosci. 4:234.

Pereira F, Mitchell T, Botvinick MM. 2009. Machine learning classifiers and fMRI: a tutorial overview. NeuroImage. 45:S199–S209.

Pexman PM. 2008. It's Fascinating Research : The Cognition of Verbal Irony. Current Directions in Psychological Science. 17:280–290.

Polyn SM, Natu VS, Cohen JD, Norman KA. 2005. Category-specific cortical activity precedes retrieval during memory search. Science. 310:1963–1966.

Ridderinkhof KR, Ullsperger M, Crone EA, Nieuwenhuis S. 2004. The role of the medial frontal cortex in cognitive control. Science. 306:443–447.

Rilling J, Gutman D, Zeh T, Pagnoni G, Berns G, Kilts C. 2002. A neural basis for social cooperation. Neuron. 35:395–405.

Rilling JK, Sanfey AG, Aronson JA, Nystrom LE, Cohen JD. 2004. The neural correlates of theory of mind within interpersonal interactions. NeuroImage. 22:1694–1703.

Rushworth MFS, Kennerley SW, Walton ME. 2005. Cognitive neuroscience: resolving conflict in and over the medial frontal cortex. Curr Biol. 15:R54–R56.

Saur D, Kreher BW, Schnell S, Kümmerer D, Kellmeyer P, Vry M-S, Umarova R, Musso M, Glauche V, Abel S, Huber W, Rijntjes M, Hennig J, Weiller C. 2008. Ventral and dorsal pathways for language. Proc Natl Acad Sci USA. 105:18035–18040.

Schiller D, Freeman JB, Mitchell JP, Uleman JS, Phelps EA. 2009. A neural mechanism of first impressions. Nat Neurosci. 12:508–514.

Schurger A, Pereira F, Treisman A, Cohen JD. 2010. Reproducibility distinguishes conscious from nonconscious neural representations. Science. 327:97–99.

Seo H, Barraclough DJ, Lee D. 2009. Lateral intraparietal cortex and reinforcement learning during a mixed-strategy game. Journal of Neuroscience. 29:7278–7289.

Shamay-Tsoory SG, Aharon-Peretz J, Perry D. 2009. Two systems for empathy: a double dissociation between emotional and cognitive empathy in inferior frontal gyrus versus ventromedial prefrontal lesions. Brain. 132:617–627.

Shibata M, Toyomura A, Itoh H, Abe J-I. 2010. Neural substrates of irony comprehension: A functional MRI study. Brain Res. 1308:114–123.

Singer T, Lamm C. 2009. The social neuroscience of empathy. Ann N Y Acad Sci. 1156:81–96.

Sporns O, Honey CJ, Kötter R. 2007. Identification and classification of hubs in brain networks. PLoS ONE. 2:e1049.

Tamir DI, Mitchell JP. 2010. Neural correlates of anchoring-and-adjustment during mentalizing. Proc Natl Acad Sci USA. 107:10827–10832.

Thiebaut de Schotten M, Urbanski M, Duffau H, Volle E, Lévy R, Dubois B, Bartolomeo P. 2005. Direct evidence for a parietal-frontal pathway subserving spatial awareness in humans. Science. 309:2226–2228.

Vickery TJ, Jiang YV. 2009. Inferior parietal lobule supports decision making under uncertainty in humans. Cerebral Cortex. 19:916–925.

Wang AT, Lee SS, Sigman M, Dapretto M. 2006. Developmental changes in the neural basis of interpreting communicative intent. Soc Cogn Affect Neurosci. 1:107–121.

Watanabe T, Hirose S, Wada H, Katsura M, Chikazoe J, Jimura K, Imai Y, Machida T, Shirouzu I, Miyashita Y, Konishi S. 2011. Prediction of subsequent recognition performance using brain activity in the medial temporal lobe. NeuroImage. 54:3085–3092.

Watanabe T, Kimura HM, Hirose S, Wada H, Imai Y, Machida T, Shirouzu I, Miyashita Y, Konishi S. 2012a. Functional Dissociation between Anterior and Posterior Temporal Cortical Regions during Retrieval of Remote Memory. Journal of Neuroscience. 32:9659–9670.

Watanabe T, Yahata N, Abe O, Kuwabara H, Inoue H, Takano Y, Iwashiro N, Natsubori T, Aoki Y, Takao H, Sasaki H, Gonoi W, Murakami M, Katsura M, Kunimatsu A, Kawakubo Y, Matsuzaki H, Tsuchiya KJ, Kato N, Kano Y, Miyashita Y, Kasai K,

Yamasue H. 2012b. Diminished Medial Prefrontal Activity behind Autistic Social Judgments of Incongruent Information. PLoS ONE. 7:e39561.

Williams ZM, Bush G, Rauch SL, Cosgrove GR, Eskandar EN. 2004. Human anterior cingulate neurons and the integration of monetary reward with motor responses. Nat Neurosci. 7:1370–1375.

Winston JS, Strange BA, O'Doherty J, Dolan RJ. 2002. Automatic and intentional brain responses during evaluation of trustworthiness of faces. Nat Neurosci. 5:277–283.

Wittfoth M, Schröder C, Schardt DM, Dengler R, Heinze H-J, Kotz SA. 2010. On emotional conflict: interference resolution of happy and angry prosody reveals valence-specific effects. Cerebral Cortex. 20:383–392.

Xue G, Mei L, Chen C, Lu Z-L, Poldrack RA, Dong Q. 2011. Spaced learning enhances subsequent recognition memory by reducing neural repetition suppression. J Cogn Neurosci. 23:1624–1633.

Yamasaki S, Yamasue H, Abe O, Suga M, Yamada H, Inoue H, Kuwabara H, Kawakubo Y, Yahata N, Aoki S, Kano Y, Kato N, Kasai K. 2010. Reduced gray matter volume of pars opercularis is associated with impaired social communication in high-functioning autism spectrum disorders. Biol Psychiatry. 68:1141–1147.

Yamasue H, Abe O, Suga M, Yamada H, Inoue H, Tochigi M, Rogers M, Aoki S, Kato N, Kasai K. 2008. Gender-common and -specific neuroanatomical basis of human anxiety-related personality traits. Cerebral Cortex. 18:46–52.

Zaki J, Hennigan K, Weber J, Ochsner KN. 2010. Social cognitive conflict resolution: contributions of domain-general and domain-specific neural systems. Journal of Neuroscience. 30:8481–8488.

Zaki J, Ochsner K. 2009. The need for a cognitive neuroscience of naturalistic social cognition. Ann N Y Acad Sci. 1167:16–30.

Zuo X-N, Ehmke R, Mennes M, Imperati D, Castellanos FX, Sporns O, Milham MP. 2011. Network Centrality in the Human Functional Connectome. Cerebral Cortex.

Figure Legends

Figure 1.

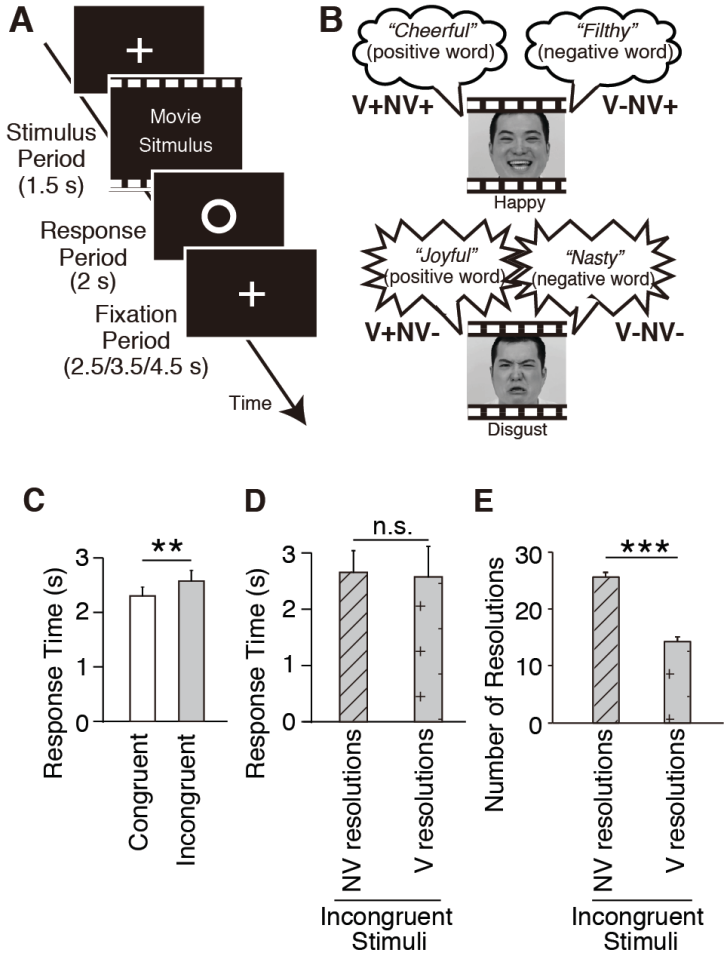

Fig. 1. Task Design and Behavioral Results.

A. Task design. In each trial during fMRI scanning, a 1.5 s video stimulus was presented with audio. The subjects were instructed to freely judge whether a professional actor who appeared in the video was a friend or foe by pressing a different button in the following 2 s response period. The average duration of a single trial was 7 s.

B. Types of video stimuli. In each video stimulus, 1 of 20 professional actors spoke an emotional word (positive or negative verbal information) with an emotional facial expression

and voice prosody (positive or negative nonverbal information).

C. Differences in response time between congruent and incongruent stimuli. Responses to incongruent stimuli were significantly longer than responses to congruent stimuli (**: $P < 0.01$, paired t-test).

D. Difference in response time between nonverbal-cue-biased and verbal-cue-biased resolutions. Friend/foe judgments of incongruent stimuli were classified into nonverbal-cue-biased or verbal-cue-biased resolutions of incongruence (see Introduction). There was no significant difference in response time between nonverbal-cue-biased and verbal-cue-biased resolutions.

E. Difference in the number of incongruent resolutions. Participants made significantly more nonverbal-cue-biased resolutions than verbal-cue-biased resolutions (***: $P < 0.001$, paired t-test).

Figure 2

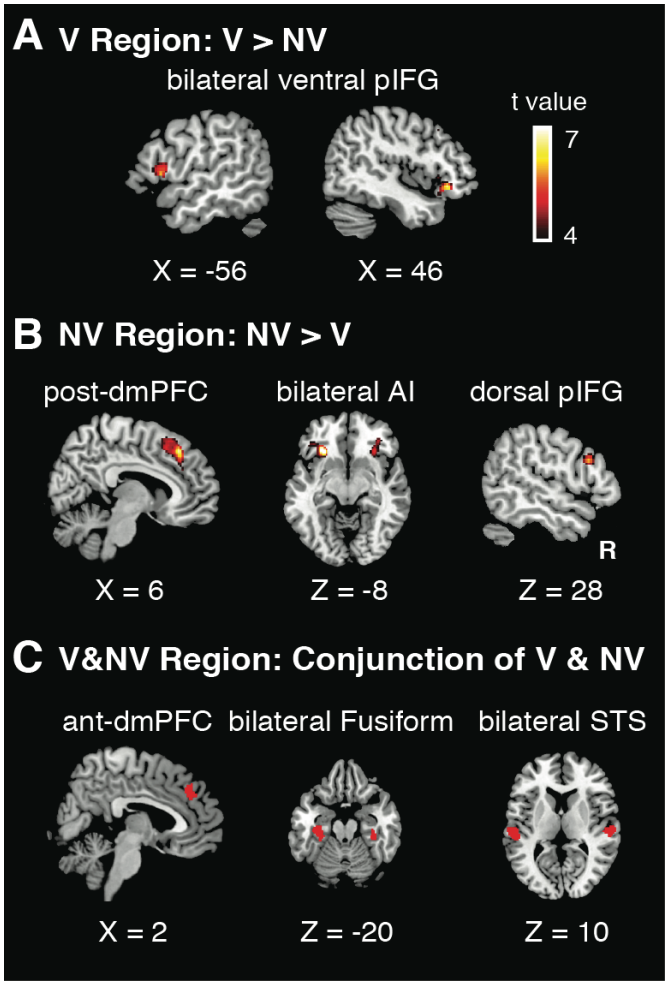

Fig. 2. Brain regions related to V and NV resolutions.

A. Brain regions specific to V resolutions. The bilateral ventral posterior inferior frontal gyrus (pIFG) showed significantly larger activity during V resolutions than during NV resolutions ($P < 0.05$, FDR-corrected).

B. Brain regions specific to NV resolutions. The posterior dorsal medial prefrontal cortex (post-dmPFC), bilateral anterior insula (AI), and dorsal pIFG showed significantly larger activity during NV resolutions than during V resolutions ($P < 0.05$, FDR-corrected).

C. Brain regions common to V and NV resolutions. Conjunction analysis of V resolutions ($P < 0.001$, uncorrected) and NV resolutions ($P < 0.001$, uncorrected) revealed brain regions common to V and NV resolutions ($P < 10^{-6}$, uncorrected). The regions include the anterior dmPFC, bilateral fusiform gyrus, and bilateral superior temporal sulcus (STS).

Figure 3

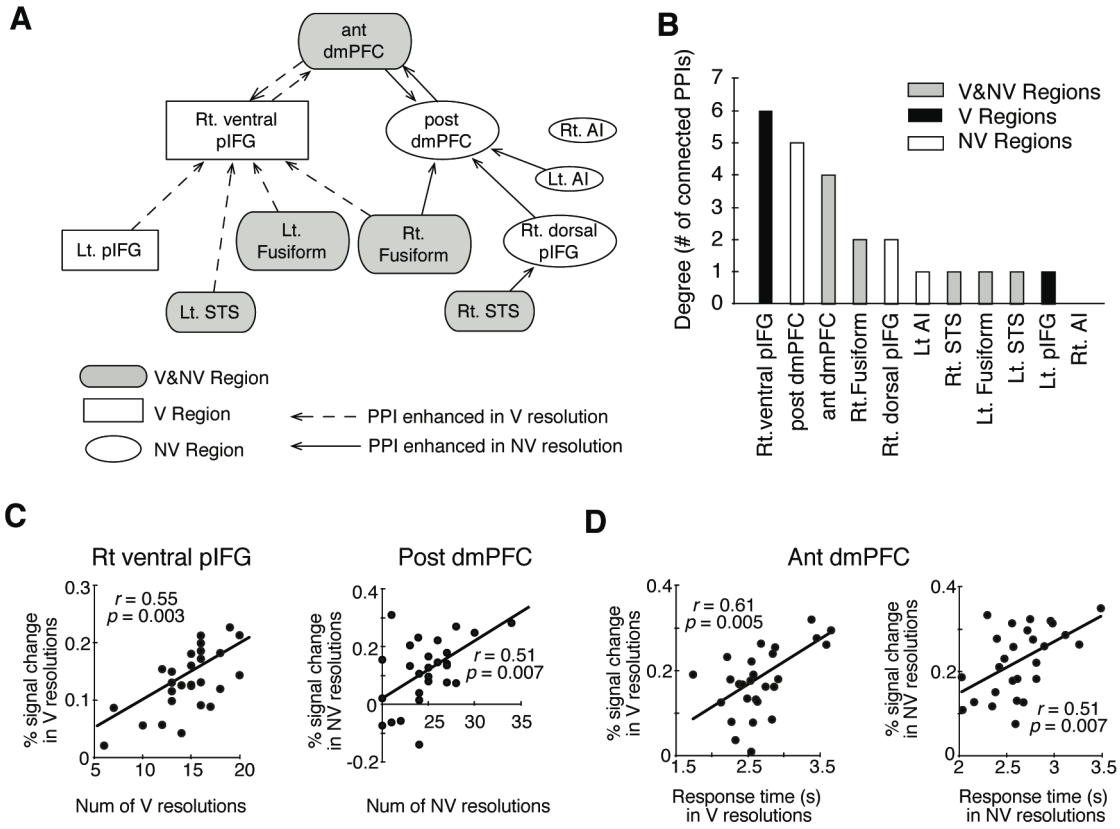

Fig. 3. PPI-based networks and comparison with behavioral pattern.

A. PPI-based network topology. The solid arrows show PPIs enhanced during the NV resolutions compared to during V resolutions, whereas the dashed arrows indicate PPIs enhanced during the V resolutions ($P < 0.05$, FDR-corrected, Table 2). The boxes show the V Regions, the circles the NV Regions, and the gray boxes the V&NV Regions.

B. Degree distribution. The bars show the number of the significantly enhanced PPIs for each of the regions. The right ventral pIFG had the largest degree (i.e., the largest number of significant PPIs). The post-dmPFC had the largest degree among NV Regions, and the ant-dmPFC had the largest degree among V&NV Regions.

C. Comparison between the brain activity and the tendency of conflict resolutions. Left panel: Among the V Regions, only the right ventral pIFG showed the significant positive correlation

between its brain activity and the number of V resolutions ($P < 0.05$, Bonferroni-corrected). Right panel: Among the NV Regions, only the post-dmPFC showed the significant positive correlation between its brain activity and the number of NV resolutions ($P < 0.05$, Bonferroni-corrected).

D. Comparison between the brain activity and the response time. Among the V&NV Regions, only the ant-dmPFC showed significant positive correlations between its brain activity and the response time spent for conflict resolutions ($P < 0.05$, Bonferroni-corrected).

Figure 4

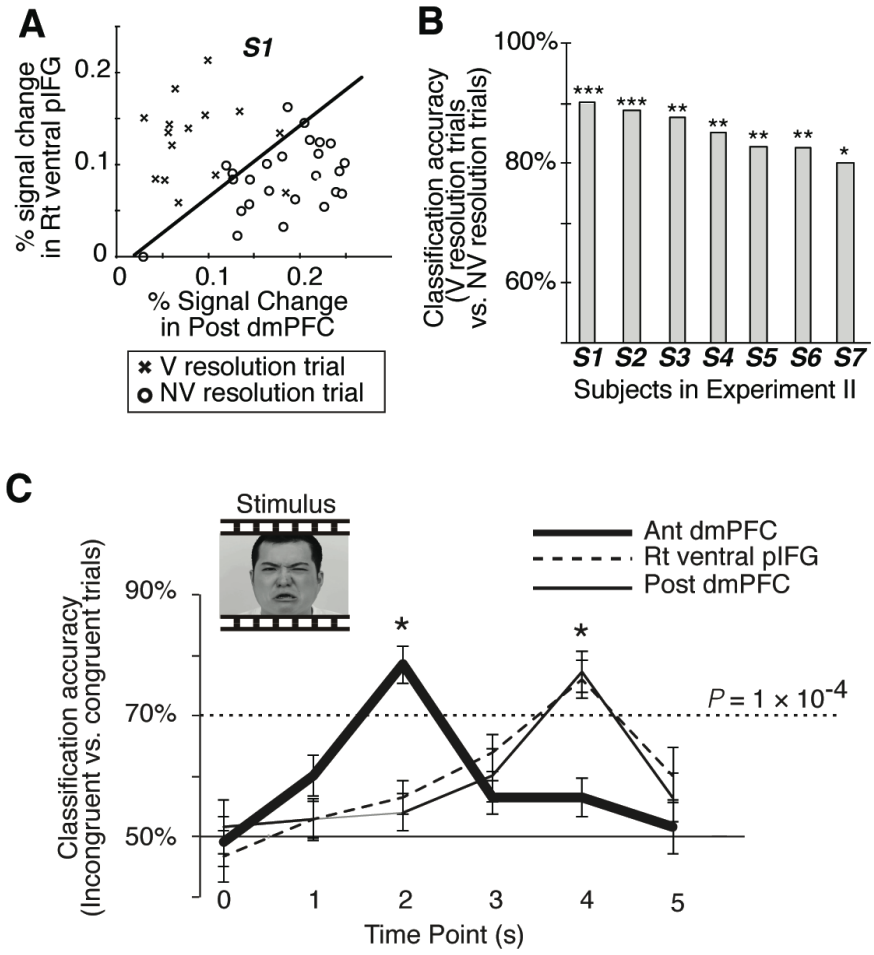

Fig. 4. Characterization of the central regions based on MVPA.

A. Representative result of the MVPA using the brain activity in the resolution-type-specific hub regions. In the case of one of the subjects in the fMRI experiment II (S1), the MVPA using brain activity of resolution-type-specific hub regions accurately predicted whether the subjects chose a V or NV resolution in response to the incongruent stimulus (90%, $P < 0.001$ in a permutation test).

B. MVPA results in all the seven subjects. The MVPA using the brain activity in the resolution-type-specific hub regions predicted types of conflict resolutions (V or NV resolutions) in all the seven subjects in the fMRI experiment II (*: $P < 0.05$; ** $P < 0.01$; *** $P < 0.001$).

C. Comparison of time courses of classification accuracy among the three central regions.

Another MVPA estimated which time period had the largest information about the difference between the congruent and incongruent stimuli trials. For the ant-dmPFC, the classification accuracy peaked at 2 s after the stimulus onset, whereas, for the post-dmPFC or right ventral pIFG peaked at 4 s after the stimulus onset ($P < 1 \times 10^{-4}$ in a permutation test). * shows the time period during which there was significant difference in the classification accuracy between the ant-dmPFC and post-dmPFC/right ventral pIFG ($P < 0.05$, Bonferroni-corrected, in a paired t-test). Error bars: s.d.